

## **A tactile sensor using single layer graphene for surface texture recognition**

Sungwoo Chun<sup>1</sup>, Yeonhai Choi<sup>1</sup>, Dong Ik Suh<sup>1</sup>, Gi Yoon Bae<sup>1</sup>, Sangil Hyun<sup>2</sup> and Wanjun Park<sup>1,\*</sup>

<sup>1</sup> Department of Electronics Engineering, Hanyang University, Seoul 133-791 South Korea

<sup>2</sup> Computer Aided Science & Engineering Lab., Korea Institute of Ceramic Engineering & Technology (KICET), Jinju 52851 South Korea

**\*Corresponding author:** E-mail: [wanjun@hanyang.ac.kr](mailto:wanjun@hanyang.ac.kr), Tel: +82-2-2220-4315

## Supplementary Information S1: Basic characteristics of single layer graphene

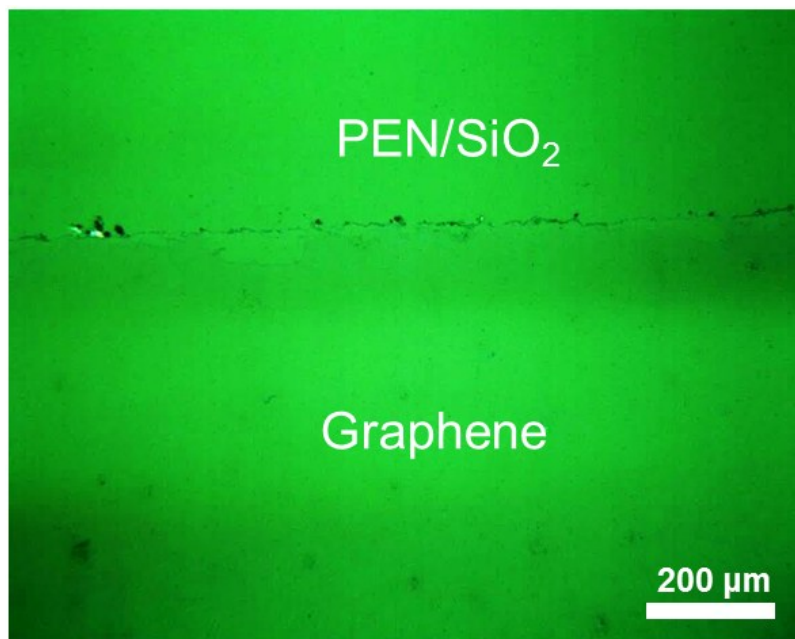


**Figure S1-1.** Optical image of SLG transferred onto SiO<sub>2</sub>-coated PEN substrate. The SLG surface has no cracks or voids.

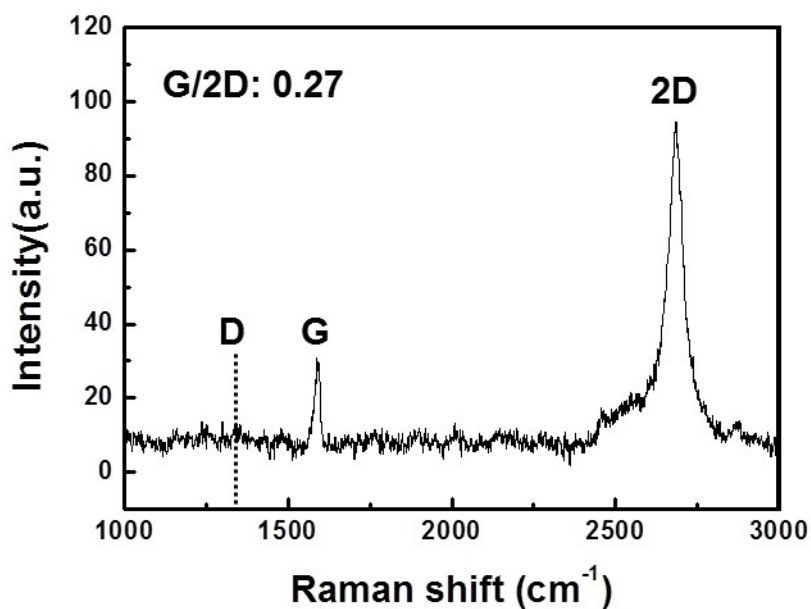


**Figure S1-2.** Raman resonance with a 514 nm laser source for graphene grown by chemical vapor deposition. This measurement was performed for graphene transferred onto SiO<sub>2</sub>-coated Si substrate. The ratio ( $\sim 0.27$ ) of intensities of the G band (1587 cm<sup>-1</sup>) to the 2D band

( $2682\text{ cm}^{-1}$ ) and absence of the D band ( $1350\text{ cm}^{-1}$ ) intensity confirms typical single-layer graphene (SLG) without defects.

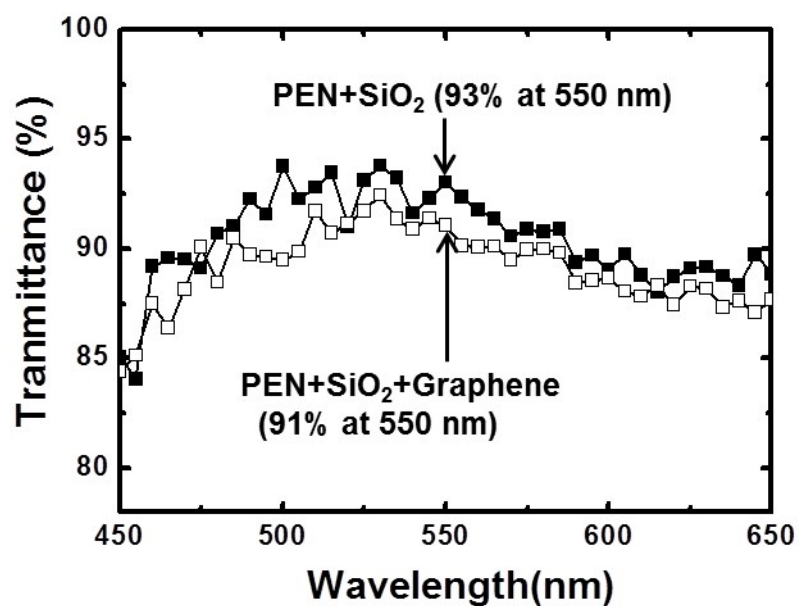
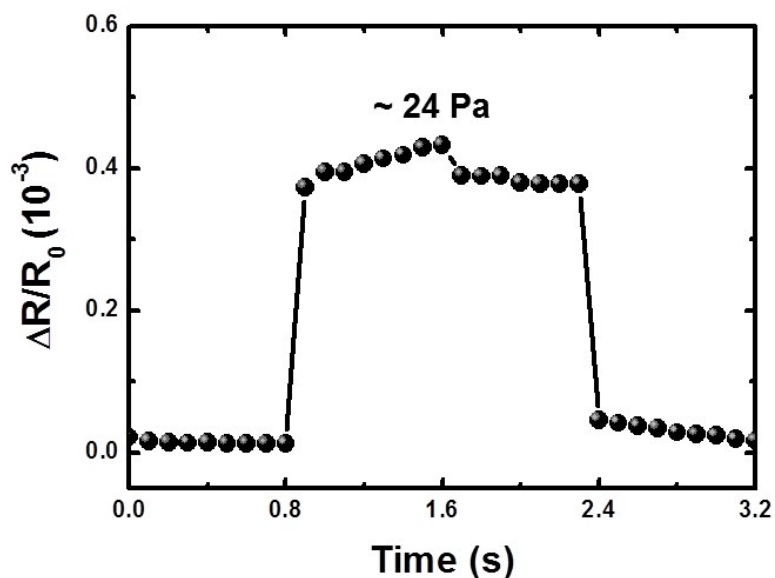
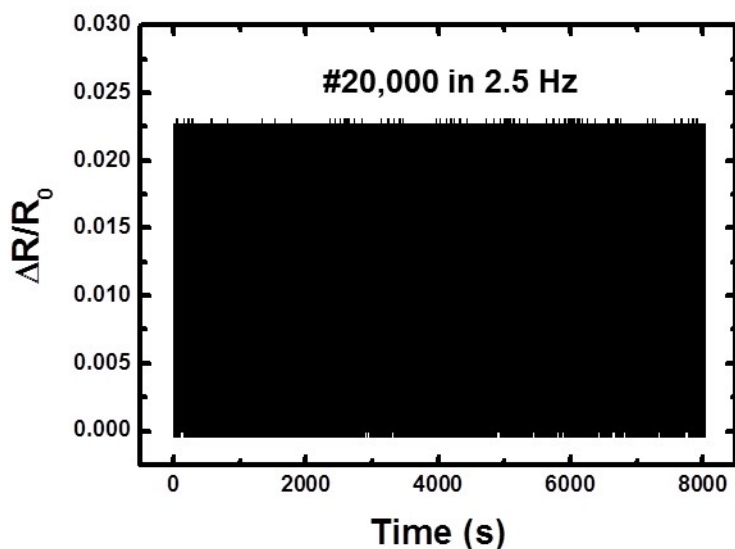


**Figure S1-3.** Transmittance curves for Graphene/SiO<sub>2</sub>/PEN. The transmittance value of 91% indicates that graphene induced a transmission loss of 2.2%, which is typical for SLG.

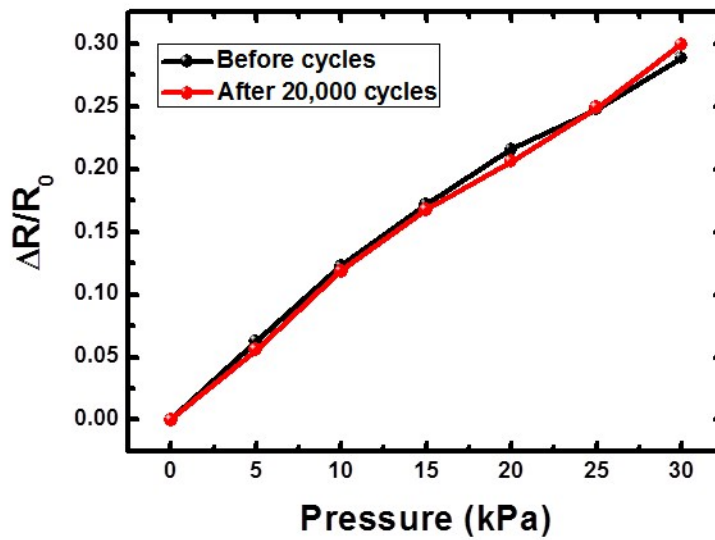
**Supplementary Information S2: Basic characteristics of single layer graphene force sensor**



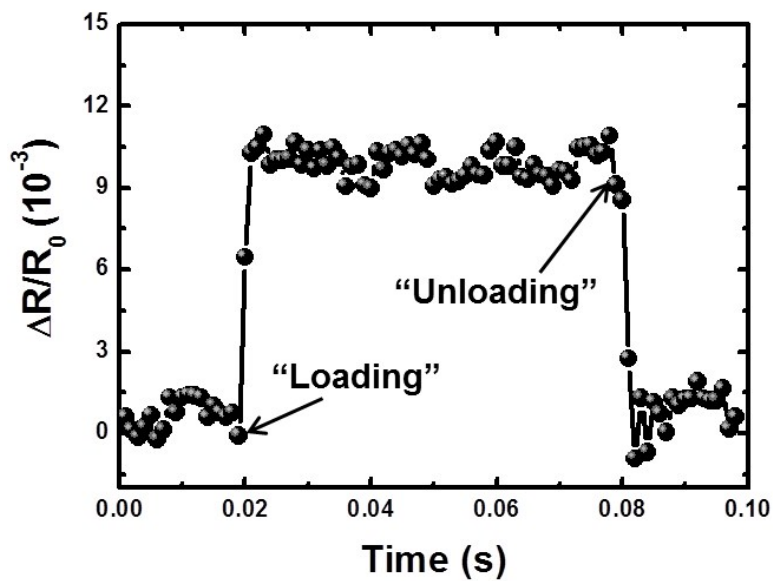
**Supplementary Figure S2-1.** Minimum detecting pressure of the sensor. The sensor is detectable for the vertical pressure as low as 24 Pa driven by a weight of 240 mg on 1 cm<sup>2</sup> contact area.



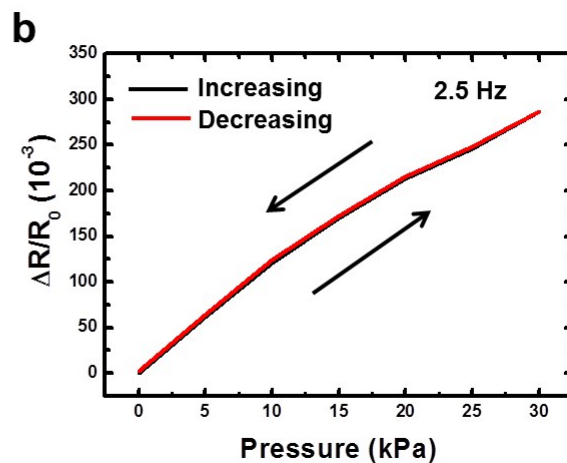
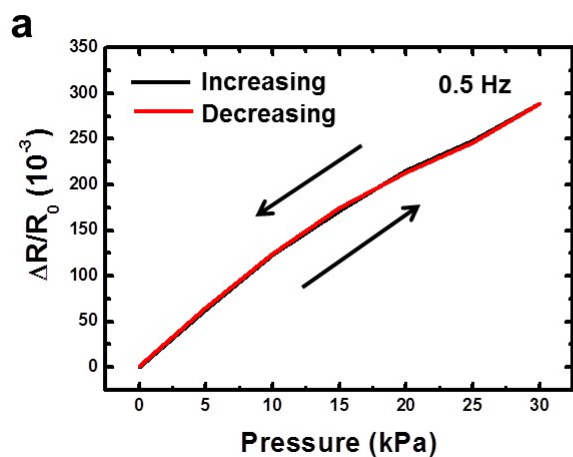
**Supplementary Figure S2-2.** Reproducible operation of the sensor. Ratio of resistance change after 20000 repetitions by loading-unloading cycles with a pulse of vertical pressure (2 kPa) for 2.5 Hz.



**Supplementary Figure S2-3.** Comparison of resistance change before and after repeated loading-unloading cycle (20,000 repetitions).

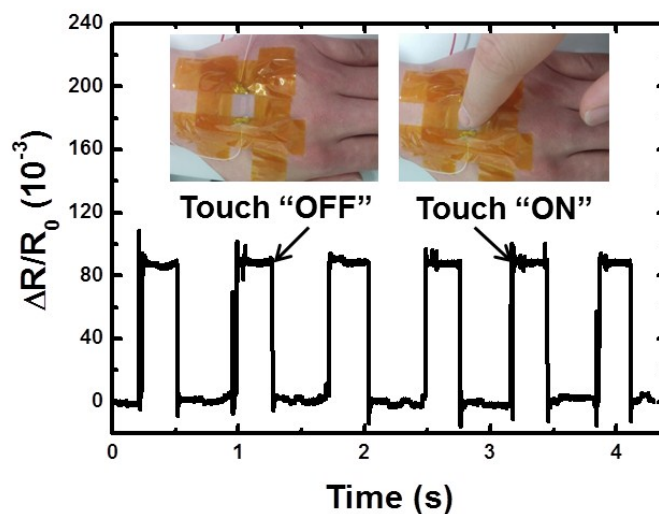


**Supplementary Figure S2-4.** Response and relaxation time of the sensor. The response time is estimated as fast as  $\sim 2$  ms for deformation and  $\sim 3$  ms for restoration with a measurement of 1 ms time interval between loading and unloading for the vertical pressure (600 Pa).

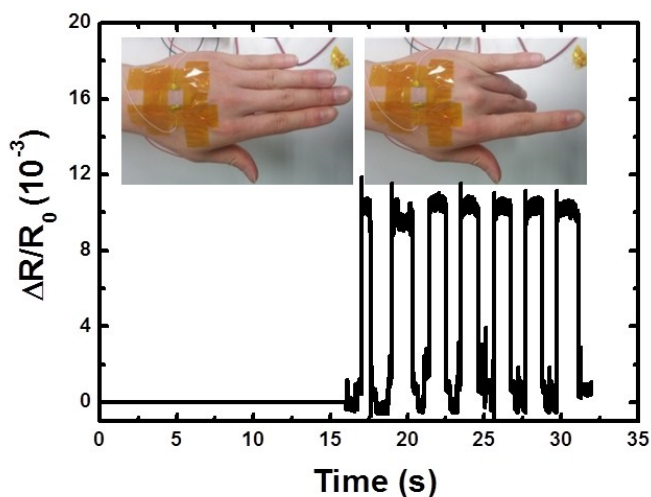


**Supplementary Figure S2-5.** Hysteresis curves with forward and backward applying pressure whose range is 0 to 30 kPa for different pulse durations (a) 0.5 Hz, and (b) 2.5 Hz.

### Supplementary Information S3: Demonstration of a flexible force sensor

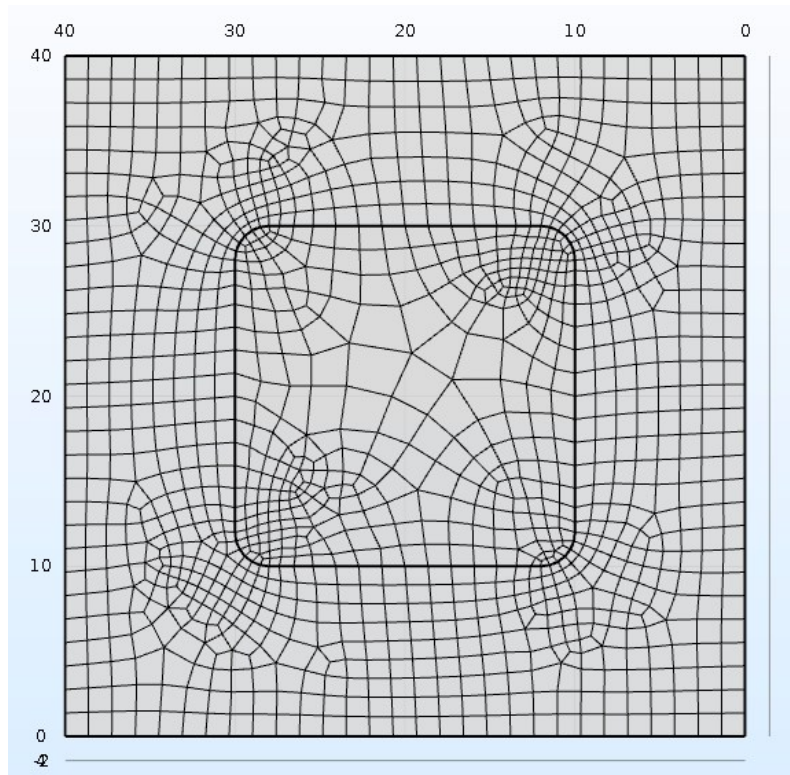


**Supplementary Figure S3-1.** Demonstration for a switch equipped on skin. The gentle touching with index finger was carried out to generate an actual human touching for six times. The result shows the output signals with the relative resistance change of  $\sim 0.09$ . It indicates that the amount of the touching corresponds to  $\sim 7$  kPa.



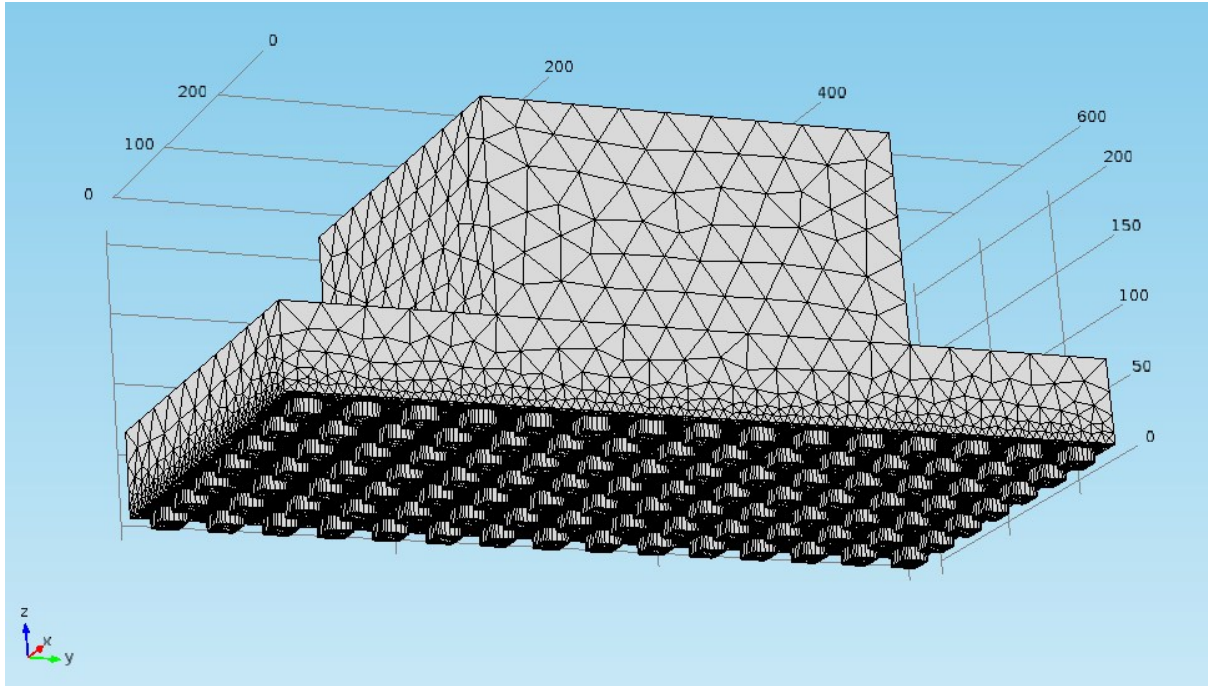
**Supplementary Figure S3-2.** The sensor equipped on skin. Internal pressure associated with finger bending was evaluated with the sensor attached to the back side of the hand. The pressure associated with finger bending was estimated to be 550 Pa.

## Supplementary Information S4: Sensor geometry for FEM calculations



**Supplementary Figure S4-1.** The unit cell repeated in array formation to form a complete PAS. Structural periodicity was imposed in planar orientations. The solid square inside the cell shows the micro-structure of the PAS with a contact area ratio ( $\phi$ ) of 0.25 corresponding to the PAS of the actual sensor. Finite element mesh consisted of 5,812 elements and 4,808 nodes.





**Supplementary Figure S4-2.** Extended unit cell of the AFPS used in FEM calculations. The line pattern of the AFPS covered seven rows of the PAS array. The sensor was completed by repetition of the extended unit cell with structural periodicity in planar orientations.

**Supplementary Table 1.** Material parameters for FEM calculations. In this simulation on the deformation of graphene sheet under the vertical pressure, we used an artificial properties of the graphene sheet equal (or more compliant) to the PEN film because we assumed the graphene films can deform exactly same with the PEN part.

Phase	Young's modulus (GPa)	Poisson ratio
<b>PET (Film)</b>	2.0	0.3
<b>PEN (Film)</b>	5.0	0.3
<b>SiO<sub>2</sub></b>	70	0.3